Inorg. Chem. **2009**, *48*, 3000−3011

Synthesis and Redox Chemistry of High-Valent Uranium Aryloxides

Skye Fortier, Guang Wu, and Trevor W. Hayton*

Department of Chemistry and Biochemistry, University of California Santa Barbara, California 93106

Received November 25, 2008

Alcoholysis of $U(O^tBu)_6$ with 1 or 2 equiv of C_6F_5OH generates $U(O^tBu)_5(OC_6F_5)$ (**1**) and $U(O^tBu)_4(OC_6F_5)_2$ (**2**) in 70% and 65% yields, respectively. Complexes **1** and **2** have been fully characterized, and their solution redox properties have been determined by cyclic voltammetry. Complex **1** exhibits a reversible reduction feature at $E_{1/2} = -0.60$ V (vs $[Cp_2Fe]^{0/+}$), while **2** exhibits a reversible reduction feature at −0.24 V (vs $[Cp_2Fe]^{0/+}$). Attempts to isolate the other *tert*-butoxide/pentafluorophenoxide complexes, $U(O^tBu)_{6-n}(OC_6F_5)_n$ ($n = 3-6$), did not generate the intended products. For instance, reaction of $U(O^tBu)_6$ with 6 equiv of C_6F_5OH in CH_2Cl_2 results in the formation $[Li(HO^tBu)_2][U(OC_6F_5)_6]$ (**3**). The source of the lithium cation in **3** is likely LiI, which is present from the initial synthesis of the $U(O^tBu)_6$. However, reaction of LiI-free $U(O^tBu)_6$ with 6 equiv of C_6F_5OH results in the formation of a uranyl complex, $UO_2(OC_6F_5)_2(HO^tBu)_2$ (**4**), along with isobutylene and $^tBuOC_6F_5$. To probe the mechanism of this transformation, $U(O^tBu)_6$ was reacted with $C_6F_5{}^{18}OH \cdot 0.5DME$. This produces $UO_2(^{18}OC_6F_5)_2(DME)$ (**5-^{18}O**) along with $^tBu^{18}OC_6F_5$ as determined by GC/MS, which suggests that oxo formation only occurs by *tert*-butyl cation elimination and not aromatic nucleophilic substitution. Several other synthetic pathways to $U^{VI}(OC_6F_5)_6$ were also investigated. Thus, addition of 10 equiv of C_6F_5OH to $[Li(THF)]_2[U(O^tBu)_6]$ in Et_2O followed by addition of DME results in the formation of $[Li(DME)_3]_2[U(OC_6F_5)_6]$ (**7**). Oxidation of **7** with 2 equiv of AgOTf in CH_2Cl_2 or toluene generates $[Li(DME)_3][U(OC_6F_5)_6]$ (**8**) or $[Ag(\eta^2\text{-}C_7H_8)_2(DME)][U(OC_6F_5)_6]$ (**9**), respectively. However, no evidence for the formation of $U^{VI}(OC_6F_5)_6$ was observed during these reactions.

Introduction

An improved understanding of the bonding in the actinides has the potential to affect the extractants and processes chosen for the next generation of the nuclear fuel cycle.[1−4] For example, ligand sets possessing soft-donor atoms display a greater selectivity for curium and americium ions vs the lanthanide ions found in spent nuclear fuel.[5−7] This selectivity has been exploited in the development of new ligands[8−11] and has been rationalized by an increased covalency in the An−L bonds, relative to their Ln−L counterparts.[5,12−15] This favors the coordination of polarizable donor atoms, such as N and S, and is probably the result of the greater spatial extension of the 5f and 6d orbitals.[14,16] The enhancement of covalency in the actinides over the lanthanides has also been observed in a comparison of metal−ligand bond lengths for $M[(EP^iPr_2)_2N]_3$ (M = U, Pu, La, and Ce; E = S, Se, and Te),[12,17] $M(SMes^*)_3$ (M = U, La, Ce, and Pr),[18] and

* To whom correspondence should be addressed. E-mail: hayton@chem.ucsb.edu

(1) Ansoborlo, É.; Amekraz, B.; Moulin, C; Moulin, V.; Taran, F.; Bailly, T.; Burgada, R.; Hengé-Napoli, M.-H.; Jeanson, A.; Den Auwer, C.; Bonin, L.; Moisy, P. *C. R. Chim.* **2007**, *10*, 1010–1019.
(2) Madic, C.; Lecomte, M.; Baron, P.; Boullis, B. *C. R. Phys.* **2002**, *3*, 797–811.
(3) Mathur, J. N.; Murali, M. S.; Nash, K. L. *Solv. Extr. Ion Exch.* **2001**, *19*, 357–390.
(4) Katz, J. J.; Seaborg, G. T.; Morss, L. R. *The Chemistry of the Actinide Elements*, 2nd ed.; Chapman and Hall: New York, 1986; Vol. 1.
(5) Jensen, M. P.; Bond, A. H. *J. Am. Chem. Soc.* **2002**, *124*, 9870–9877.
(6) Guoxin, T.; Yongjun, Z.; Jingming, X.; Ping, Z.; Tiandou, H.; Yaning, X.; Jing, Z. *Inorg. Chem.* **2003**, *42*, 735–741.
(7) Binnemans, K. *Chem. Rev.* **2007**, *107*, 2592–2614.
(8) Drew, M. G. B.; Foreman, M. R. S. J.; Hill, C.; Hudson, M. J.; Madic, C. *Inorg. Chem. Commun.* **2005**, *8*, 239–241.
(9) Drew, M. G. B.; Hudson, M. J.; Youngs, T. G. A. *J. Alloys Compd.* **2004**, *374*, 408–415.
(10) Kolarik, Z. *Chem. Rev.* **2008**, *108*, 4208–4252.
(11) Stumpf, S.; Billard, I.; Gaillard, C.; Panak, P. J.; Dardenne, K. *Inorg. Chem.* **2008**, *47*, 4618–4626.
(12) Gaunt, A. J.; Reilly, S. D.; Enriquez, A. E.; Scott, B. L.; Ibers, J. A.; Sekar, P.; Ingram, K. I. M.; Kaltsoyannis, N.; Neu, M. P. *Inorg. Chem.* **2008**, *47*, 29–41.
(13) Mazzanti, M.; Wietzke, R.; Pecaut, J.; Latour, J. M.; Maldivi, P.; Remy, M. *Inorg. Chem.* **2002**, *41*, 2389–2399.
(14) Choppin, G. R. *J. Alloys Compd.* **2002**, *344*, 55–59.
(15) Miguirditchian, M.; Guillaneux, D.; Guillaumont, D.; Moisy, P.; Madic, C.; Jensen, M. P.; Nash, K. L. *Inorg. Chem.* **2005**, *44*, 1404–1412.
(16) Ionova, G.; Ionov, S.; Rabbe, C.; Hill, C.; Madic, C.; Guillaumont, R.; Krupa, J. C. *Solv. Extr. Ion Exch.* **2001**, *19*, 391–414.

10.1021/ic802266y CCC: $40.75
Published on Web 02/26/2009

$[M(Cp^*)(SBT)_3]^-$ (M = U, La, Ce, and Nd; SBT = 2-mercapto benzothiolate).[19] Other evidence for covalency in actinide−ligand bonding comes from the comprehensive theoretical and experimental study of the uranyl ion over the past decade,[20−22] and more recently, the DFT analysis of the bonding in the imido analogue of the uranyl ion, $[RN{=}U{=}NR]^{2+}$.[23]

However, there is still much debate about the magnitude and prevalence of covalency in the actinides. For instance, comparison of the XANES spectra of curium coordinated to phosphinic and thiophosphinic acid reveals no substantial increase in the contribution of the d orbitals to metal−ligand bonding.[5] In another example, the large U−O−C_α angle of uranium alkoxides, which has been used as evidence for π-donation by the alkoxide ligand,[24−28] may simply be a manifestation of the electrostatic repulsion between M and C_α.[29] Finally, several studies have shown that DFT can overestimate metal−ligand orbital interactions,[30,31] casting doubt on calculations that show 5f and 6d participation in actinide bonding.

In this contribution, we report our efforts to understand the metal−ligand bonding in a series of uranium(VI) aryloxide complexes, namely $U(O^tBu)_5(OC_6F_5)$, $U(O^tBu)_4(OC_6F_5)_2$, and $U(O^tBu)_2(OC_6F_5)_4$. In addition, we describe our attempts to isolate the homoleptic aryloxide complex $U(OC_6F_5)_6$ by two different routes: (1) complete ligand exchange of $U(O^tBu)_6$ with C_6F_5OH, and (2) oxidation of $[Li(DME)_3]_2[U^{IV}(OC_6F_5)_6]$ and $[Li(DME)_3][U^{V}(OC_6F_5)_6]$. We have chosen to study this class of compounds because the high charge/size ratio of the U^{6+} ion should maximize covalency.[32,33] U^{6+} complexes that do not contain the dioxo ligand set of the uranyl ion are quite rare, and the study of these non-uranyl complexes could provide an important contrast to the uranyl ion in regards to the participation of the 5f and 6d orbitals.

The stabilization of the 6+ oxidation state in uranium typically requires ligands capable of strong π-donation, such as imido or oxo groups,[34−39] or electron-withdrawing halides or pseudohalides, such as in UF_6, UCl_6, and $U(OTeF_5)_6$.[40] The largest class of nonuranyl uranium(VI) compounds belongs to the $U(OR)_6$ alkoxides.[28,41−44] Despite their being known since the Manhattan project,[41] very little structural data have been collected for these compounds. In fact, only $U(OMe)_6$,[43] $U[OCH_2C(CH_3)_3]_6$,[44] and $U(O^tBu)_6$[28] have been structurally characterized. Interestingly, these complexes possess large U−O−C bond angles, suggestive of strong π-donation to the metal center.[24−27,45−48] In contrast to the uranium(VI) alkoxides, only one uranium(VI) aryloxide complex has been isolated, namely $U(^tBu\text{-calix[6]arene})_2$,[49] and it remains to be determined whether aryloxides can systematically stabilize the 6+ oxidation state of uranium. Aryloxides are typically considered poorer π-donors than alkoxides, in part because of conjugation of the oxygen p orbitals with the aromatic system.[24,45−47,50,51]

Results and Discussion

Addition of 1 equiv of C_6F_5OH to $U(O^tBu)_6$ in hexanes results in formation of a dark-red solution containing $U(O^tBu)_5(OC_6F_5)$ (**1**) over the course of several days (eq 1). Similarly, addition of 2 equiv of C_6F_5OH to $U(O^tBu)_6$ in hexanes results in the formation of $U(O^tBu)_4(OC_6F_5)_2$ (**2**) (eq 1). However, this latter transformation reaches completion in only a few hours. For either reaction mixture, removal of the solvent produces a dark-red solid which is soluble in

(17) Ingram, K. I. M.; Tassell, M. J.; Gaunt, A. J.; Kaltsoyannis, N. *Inorg. Chem.* **2008**, *47*, 7824–7833.
(18) Roger, M.; Barros, N.; Arliguie, T.; Thuery, P.; Maron, L.; Ephritikhine, M. *J. Am. Chem. Soc.* **2006**, *128*, 8790–8802.
(19) Roger, M.; Belkhiri, L.; Arliguie, T.; Thuery, P.; Boucekkine, A.; Ephritikhine, M. *Organometallics* **2008**, *27*, 33–42.
(20) Denning, R. G.; Green, J. C.; Hutchings, T. E.; Dallera, C.; Tagliaferri, A.; Giarda, K.; Brookes, N. B.; Braicovich, L. *J. Phys. Chem.* **2002**, *117*, 8008–8020.
(21) Denning, R. G. *J. Phys. Chem. A* **2007**, *111*, 4125–4143.
(22) Kaltsoyannis, N. *Inorg. Chem.* **2000**, *39*, 6009–6017.
(23) Hayton, T. W.; Boncella, J. M.; Scott, B. L.; Batista, E. R.; Hay, P. J. *J. Am. Chem. Soc.* **2006**, *128*, 10549–10559.
(24) Bradley, D. C.; Mehrotra, R. C.; Rothwell, I. P.; Singh, A. *Alkoxo and Aryloxo Derivatives of Metals*; Academic Press: San Diego, CA, 2001.
(25) Marks, T. J.; Bursten, B. E.; Casarin, M.; Ellis, D. E.; Fragala, I. *Inorg. Chem.* **1986**, *25*, 1257–1261.
(26) Cotton, F. A.; Marler, D. O.; Schwotzer, W. *Inorg. Chem.* **1984**, *23*, 4211–4215.
(27) Gulino, A.; Di Bella, S.; Fragala, I.; Casarin, M.; Seyam, M. A.; Marks, T. J. *Inorg. Chem.* **1993**, *32*, 3873–3879.
(28) Fortier, S.; Wu, G.; Hayton, T. W. *Inorg. Chem.* **2008**, *47*, 4752–4761.
(29) Russo, M. R.; Kaltsoyannis, N.; Sella, A. *Chem. Commun.* **2002**, 2458–2459.
(30) Atanasov, M.; Daul, C.; Gudel, H. U.; Wesolowski, T. A.; Zbiri, M. *Inorg. Chem.* **2005**, *44*, 2954–2963.
(31) Szilagyi, R. K.; Metz, M.; Solomon, E. I. *J. Phys. Chem. A* **2002**, *106*, 2994–3007.
(32) Sievers, R. E.; Bailar, J. C. J. *Inorg. Chem.* **1962**, *1*, 174–182.
(33) Frenking, G.; Pidun, U. *Dalton Trans.* **1997**, 1653–1662.
(34) Burns, C. J.; Smith, W. H.; Huffman, J. C.; Sattelberger, A. P. *J. Am. Chem. Soc.* **1990**, *112*, 3237–3239.
(35) Arney, D. S. J.; Burns, C. J.; Smith, D. C. *J. Am. Chem. Soc.* **1992**, *114*, 10068–10069.
(36) Arney, D. S. J.; Burns, C. J. *J. Am. Chem. Soc.* **1995**, *117*, 9448–9460.
(37) Hayton, T. W.; Boncella, J. M.; Scott, B. L.; Palmer, P. D.; Batista, E. R.; Hay, P. J. *Science* **2005**, *310*, 1941–1943.
(38) Hayton, T. W.; Boncella, J. M.; Scott, B. L.; Batista, E. R. *J. Am. Chem. Soc.* **2006**, *128*, 12622–12623.
(39) Brown, D.; Denning, R. G.; Jones, R. H. *Chem. Commun.* **1994**, 2601–2602.
(40) Templeton, L. K.; Templeton, D. H.; Bartlett, N.; Seppelt, K. *Inorg. Chem.* **1976**, *15*, 2720–2722.
(41) Gilman, H.; Jones, R. G.; Bindschadler, E.; Blume, D.; Karmas, G.; Martin, G. A., Jr.; Thirtle, J. R.; Yeoman, F. A. *J. Am. Chem. Soc.* **1956**, *78*, 6030–6032.
(42) Bradley, D. C.; Chatterjee, A. K.; Chatterjee, A. K. *J. Inorg. Nucl. Chem.* **1959**, *12*, 71–79.
(43) Marks, T. J.; Cuellar, E. A. *J. Am. Chem. Soc.* **1983**, *205*, 4580–4589.
(44) Wilkerson, M. P.; Burns, C. J.; Dewey, H. J.; Martin, J. M.; Morris, D. E.; Paine, R. T.; Scott, B. L. *Inorg. Chem.* **2000**, *39*, 5277–5285.
(45) Barron, A. R. *Polyhedron* **1995**, *14*, 3197–3207.
(46) Healy, M. D.; Power, M. B.; Barron, A. R. *Coord. Chem. Rev.* **1994**, *130*, 63–135.
(47) Coffindaffer, T. W.; Steffy, B. D.; Rothwell, I. P.; Floting, K.; Huffman, J. C.; Streib, W. E. *J. Am. Chem. Soc.* **1989**, *111*, 4742–4749.
(48) Chisholm, M. H.; Davidson, E. R.; Huffman, J. C.; Quilan, K. B. *J. Am. Chem. Soc.* **2001**, *123*, 9652–9664.
(49) Leverd, P.; Nierlich, M. *Eur. J. Inorg. Chem.* **2000**, 1733–1738.
(50) Willis, C. J. *Coord. Chem. Rev.* **1988**, *88*, 133–202.
(51) Coffindaffer, T. W.; Rothwell, I. P.; Huffman, J. C. *Inorg. Chem.* **1983**, *22*, 2906–2910.

nonpolar solvents, such as hexanes and diethyl ether, but is insoluble in MeCN. Recrystallization from Et_2O/MeCN produces **1** or **2** as thin dark-red plates in 70% and 65% yield, respectively.

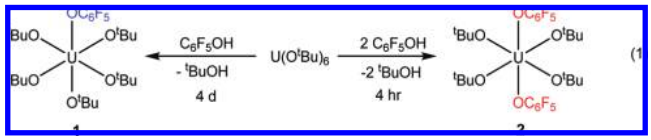

The ^{1}H NMR spectrum of **1** in C_6D_6 consists of two singlets at 1.58 and 1.60 ppm in a 4:1 ratio, assignable to the equatorial and axial *tert*-butyl groups, respectively. The ^{19}F{^{1}H} NMR spectrum of **1** displays three resonances at −97.65, −106.10, and −112.17 ppm in a 2:2:1 ratio, as anticipated for the pentafluorophenoxide substituent. The ^{1}H NMR spectrum of **2** in C_6D_6 contains a singlet at 1.57 ppm assignable to the *tert*-butyl protons, while the ^{19}F{^{1}H} NMR spectrum of **2** possesses three resonances at −98.21, −104.84, −109.42 ppm in a 2:2:1 ratio. However, a second set of resonances also appears in the ^{19}F{^{1}H} NMR spectrum of **2**, at −97.54, −105.11, −108.05 ppm. The relative ratio between these two sets of peaks is 4:1. Moreover, these peaks are always present in samples of **2** and always appear in the same relative ratio. Thus, we have assigned these resonances to the cis isomer of **2**. Consistent with this formulation, two additional singlets also appear in the ^{1}H NMR spectra of **2**, at 1.58 and 1.52 ppm in a 1:1 ratio. Single crystals of **1** or **2** suitable for a complete X-ray crystallographic analysis have remained elusive. However, a preliminary X-ray structure of **2** suggested the complex adopts the trans geometry in the solid-state, but poor data quality has precluded satisfactory refinement of the structure.

To understand the comparatively slow formation of **1**, we have monitored the alcoholysis of U(O^{t}Bu)$_6$ with 1 equiv of C_6F_5OH by ^{1}H and ^{19}F{^{1}H} NMR spectroscopy. The initial spectrum reveals the formation of complex **2**, in addition to the presence of unreacted U(O^{t}Bu)$_6$ and minor amounts of complex **1** and other unidentified species. However upon standing, complex **1** becomes the dominant product, while the relative amounts of complex **2**, U(O^{t}Bu)$_6$, and the other products decrease. Once isolated and purified, complex **2** is stable to disproportionation for at least several hours as determined by ^{19}F{^{1}H} NMR spectroscopy. We have also monitored the conproportionation of independently prepared **2** with U(O^{t}Bu)$_6$, which leads to the formation of **1** as the only product. The reaction is slow, requiring 18 days to reach 90% completion when monitored by ^{1}H and ^{19}F{^{1}H} NMR spectroscopy (eq 2). In contrast, addition of 1 equiv of C_6F_5OH to **1** immediately generates **2**.

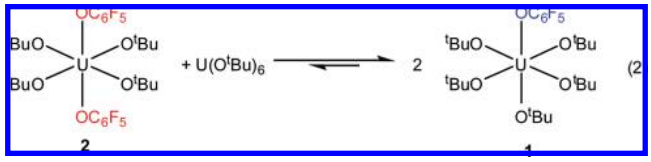

The solution phase redox properties of **1** and **2** have been measured by cyclic voltammetry. The cyclic voltammogram of **1** in CH_2Cl_2 exhibits a reversible reduction feature at

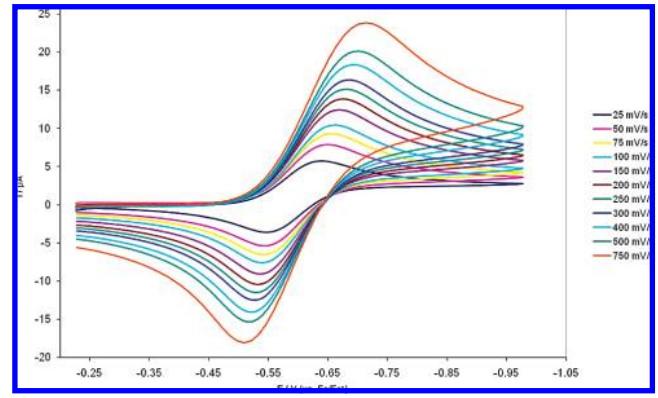

Figure 1. Room temperature cyclic voltammogram for **1** in CH_2Cl_2 vs $[Cp_2Fe]^{0/+}$ (0.1 M $[NBu_4][PF_6]$ as supporting electrolyte).

−0.60 V (vs $[Cp_2Fe]^{0/+}$) (Figure 1), which we have assigned to the U(VI)/U(V) redox couple. In addition, $i_{p,c}/i_{p,a} = 1.0$ up to scan rates of 0.75 V/s, demonstrating that the process is electrochemically reversible. A minor reduction feature is also observed in the cyclic voltammogram of **1**, at −1.12 V (vs $[Cp_2Fe]^{0/+}$), which we have attributed to the presence of small amounts of U(O^{t}Bu)$_6$.[28]

The cyclic voltammogram of **2** possesses a reversible reduction feature at −0.24 V (vs $[Cp_2Fe]^{0/+}$) in CH_2Cl_2 (see Supporting Information). We also observed a minor reduction feature at −0.69 V (vs $[Cp_2Fe]^{0/+}$), which we have assigned to trace amounts of **1** in samples of **2**. No other reduction features were observed within the range of the solvent window. Scanning to positive potentials for either **1** or **2** reveals an irreversible oxidation feature that we attribute to the removal of electrons from either the alkoxide or aryloxide ligands (see Supporting Information).

The U(VI)/U(V) reduction potentials of **1** and **2** exhibit a clear positive shift as the number of pentafluorophenoxide groups on the uranium center increases. Substitution of one *tert*-butoxide group in U(O^{t}Bu)$_6$ ($E_{1/2} = -1.12$ V vs $[Cp_2Fe]^{0/+}$)[28] to generate **1** results in a +510 mV decrease in reduction potential, and further substitution from **1** to **2** results in an additional +360 mV shift. This change in the U(VI)/U(V) redox couple demonstrates the decreased ability of the pentafluorophenoxide ligand to contribute electron density to the metal center.[50] The availability of the aryloxide lone-pair electrons for bonding may be diminished, in part, due to conjugation with the aromatic system,[24,45−48,50,51] but it also reflects the electron-withdrawing nature of the fluorine atoms on the ring. Nonetheless, the large negative reduction potentials of these and other U(VI) complexes with strong π-donor ligands[52] are good evidence for a strong π contribution to the metal−ligand bonding framework. This strong correlation between redox potential and ligand π-donating ability is common in transition metal systems.[53,54] For instance, substitution of a chloride ligand in $Ti(OAr)_2Cl_2$ (Ar = 2,6-^{t}Bu$_2$C$_6$H$_3$) with a phenoxide yields a metal center that

(52) Cummins, C. C.; Meyer, K.; Mindiola, D. J.; Baker, T. A.; Davis, W. M. *Angew. Chem., Int. Ed.* **2000**, *39*, 3063–3066.
(53) Moock, K. H.; Macgregor, S. A.; Heath, G. A.; Derrick, S.; Boeré, R. T. *Dalton Trans.* **1996**, 2067–2076.
(54) Baldas, J.; Heath, G. A.; Macgregor, S. A.; Moock, K. H.; Nissen, S. C.; Raptis, R. G. *Dalton Trans.* **1998**, 2303–2314.

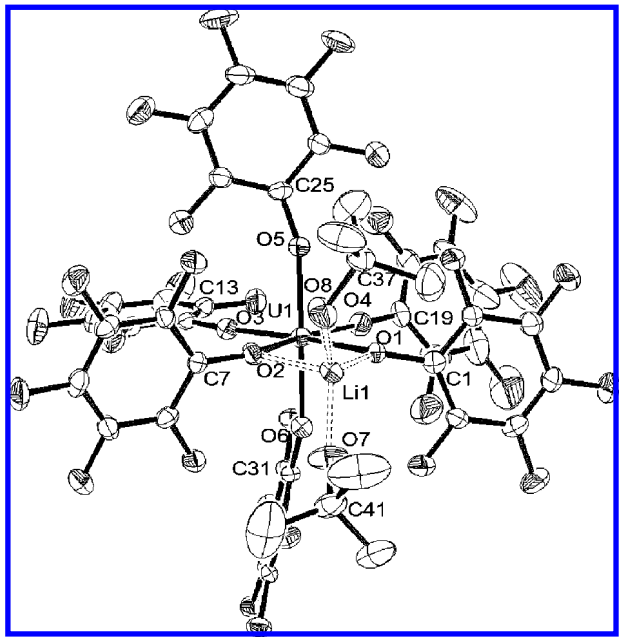

Figure 2. ORTEP diagram of $[Li(HO^tBu)_2][U(OC_6F_5)_6]$ (**3**) with 30% probability ellipsoids. Selected bond lengths (Å) and angles (deg): U1−O1 = 2.222(5), U1−O2 = 2.168(5), U1−O3 = 2.072(5), U1−O4 = 2.069(6), U1−O5 = 2.108(5), U1−O6 = 2.103(5), Li1−O1 = 2.03(2), Li1−O2 = 2.17(2), Li1−O7 = 1.86(1), Li1−O8 = 1.89(2), U1−O1−C1 = 129.2(4), U1−O2−C7 = 144.5(5), U1−O3−C13 = 170.4(5), U1−O4−C19 = 175.2(5), U1−O5−C25 = 161.7(5), U1−O6−C31 = 153.8(5), O1−U1−O2 = 78.9(2), O1−U1−O3 = 173.1(2), O1−U1−O4 = 87.8(2), O1−U1−O5 = 91.9(2), O1−U1−O6 = 87.0(2), O2−U1−O4 = 166.6(2), O2−U1−O5 = 89.2(2), O2−U1−O6 = 89.3(2), O5−U1−O6 = 178.3(2), Li1−O7−C41 = 134.8(7), Li1−O8−C37 = 132.2(7).

is 500 mV more difficult to reduce.[55,56] A related study with $W(3,5\text{-}^tBu_2cat)_{3-n}Cl_{2n}$ (n = 0, 1) reveals similar behavior.[57] These results exemplify the similarities between the transition metals and uranium and argue against a purely electrostatic interaction between uranium and oxygen in the uranium−alkoxide interaction, as has been suggested for other f element systems.[29]

Attempts to isolate the remaining *tert*-butoxide/pentafluorophenoxide complexes, i.e. $U(O^tBu)_{6-n}(OC_6F_5)_n$ (n = 3−6), did not generate the intended products. For instance, reaction of $U(O^tBu)_6$ with 6 equiv of C_6F_5OH in CH_2Cl_2 results in the formation of a deep-red reaction mixture. Slow evaporation of the solvent at −25 °C over 1 week produces small amounts of dark-red crystals. Analysis of this material by X-ray crystallography demonstrated the formation of a homoleptic uranium(V) complex, $[Li(HO^tBu)_2][U(OC_6F_5)_6]$ (**3**).

Complex **3** crystallizes in the triclinic space group $P\bar{1}$, and its solid-state molecular structure is shown in Figure 2. Complex **3** exhibits an octahedral uranium center ligated by six pentafluorophenoxide ligands. The lithium cation is coordinated by two pentafluorophenoxide ligands and two *tert*-butanol molecules, affording an overall tetrahedral geometry. The U−O bond lengths of the terminal aryloxides (U1−O3 = 2.072(5) Å, U1−O4 = 2.069(6) Å, U1−O5 = 2.108(5) Å, U1−O6 = 2.103(5) Å) and the U−O bond lengths of the bridging aryloxides (U1−O1 = 2.222(5) Å, U1−O2 = 2.168(5) Å) are comparable to those observed in $[Li(OEt_2)][U(O^tBu)_6]$ and $[U(O^iPr)_5]_2$.[26,28] The U−O−C(ipso) bond angles of the terminal aryloxides range from U1−O4−C19 = 175.2(5)° to U1−O6−C31 = 153.8(5)°, and the bridging U−O−C(ipso) bond angles are U1−O1−C1 = 129.2(4)° and U1−O2−C7 = 144.5(5)°. The Li−O(aryloxide) interactions (Li1−O1 = 2.03(2) Å, Li1−O2 = 2.17(2) Å) are typical for heterometallic alkoxides.[58] The protons of the coordinating *tert*-butanol molecules were not found during refinement of the structure, but the Li−O(*tert*-butanol) distances (Li1−O7 = 1.86(1) Å, Li1−O8 = 1.89(2) Å) and Li−O−C bond angles (Li1−O7−C41 = 134.8(7)°, Li1−O8−C37 = 132.2(7)°) are similar to those reported in other Li-HO^{t}Bu-containing complexes.[59,60]

The source of the lithium cation in **3** is probably residual LiI present from the initial synthesis of the $U(O^tBu)_6$.[28] It is likely that upon addition of C_6F_5OH to $U(O^tBu)_6$, a uranium(VI) aryloxide is formed, which is capable of oxidizing I^- to I_2. The trend in reduction potentials observed upon exchange of -O^{t}Bu with -OC_6F_5 supports this rationale. While neither **1** nor **2** would be capable of oxidizing I^-, it is possible that a uranium(VI) aryloxide with the formula $U(O^tBu)_{6-n}(OC_6F_5)_n$, where n = 3−6, would be able to effect this oxidation.[61] Complex **3** can be synthesized in a rational fashion by the addition of 6 equiv of C_6F_5OH to a toluene solution of $U(O^tBu)_6$ containing 1 equiv of LiI, where it can be isolated in 56% yield (eq 3).

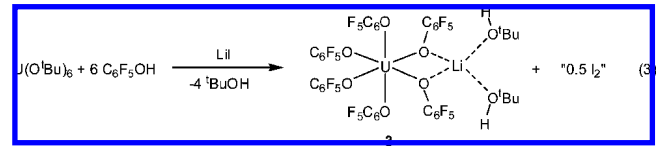

The ^{1}H NMR spectrum of **3** in CD_2Cl_2 exhibits two resonances at 1.57 and 0.95 ppm in a 1:9 ratio. These are assignable to the hydroxyl and *tert*-butyl protons of *tert*-butanol, respectively. The ^{7}Li{^{1}H} NMR spectrum in CD_2Cl_2 exhibits a singlet at 0.94 ppm. The room-temperature ^{19}F{^{1}H} NMR spectrum of **3** in CD_2Cl_2 consists of many broad and overlapping resonances. However, the addition of several equivalents of DME to these solutions results in a significant simplification of the ^{19}F{^{1}H} NMR spectrum, and three dominant peaks are observed at −99.67, −105.44, and −108.88 ppm in a 2:2:1 ratio, as anticipated for $[U(OC_6F_5)_6]^-$. In THF-d_8, these three resonances are also present however, nine other resonances are observed as well. Furthermore, a color change from dark red to bright orange

(55) Lateskey, S.; Keddington, J.; McMullen, A. K.; Rothwell, I. P.; Huffman, J. C. *Inorg. Chem.* **1985**, *24*, 995–1001.
(56) Durfee, L. D.; Latesky, S. L.; Rothwell, I. P.; Huffman, J. C.; Folting, K. *Inorg. Chem.* **1985**, *24*, 4569–4573.
(57) Beshouri, S. M.; Rothwell, I. P. *Inorg. Chem.* **1986**, *25*, 1962–1964.
(58) Pauer, F.; Power, P. P. Structures of Lithium Salts and Heteroatom Compounds. In *Lithium Chemistry: A Theoretical and Experimental Overview*; Sapse, A.-M., von Ragué Schleyer, P., Eds.; John Wiley & Sons, Inc.: New York, 1995; pp 295−392.
(59) Lambert, C.; Hampel, F.; von Ragué Schleyer, P. *Angew. Chem., Int. Ed. Engl.* **1992**, *31*, 1209–1210.
(60) Buttery, J. H. N.; Plackett, N. C.; Skelton, B. W.; Whitaker, C. R.; White, A. H. *Z. Anorg. Allg. Chem.* **2006**, *632*, 1870–1873.
(61) Connelly, N. G.; Geiger, W. E. *Chem. Rev.* **1996**, *96*, 877–910.

occurs upon dissolution of **3** in THF-d_8. These observations are consistent with the displacement of an aryloxide substituent from **3**, generating either $U(OC_6F_5)_5(HO^tBu)$ or $U(OC_6F_5)_5(THF)$. We have assigned six of these resonances at −98.69, −105.38, and −111.81 ppm and at −98.43, −104.92, and −111.52 ppm to the equatorial and axial aryloxides of $U(OC_6F_5)_5(L)$, respectively. The remaining three resonances at −98.97, −104.35, and −110.53 ppm have been assigned to the liberated $LiOC_6F_5$. Of the two possible formulations, we believe that $U(OC_6F_5)_5(HO^tBu)$ is the species generated. In support of this proposal, addition of excess ^{t}BuOH to a THF-d_8 solution of **3** results in the complete disappearance of the resonances attributed to **3**, concomitant with the growth of the resonances assigned to $U(OC_6F_5)_5(HO^tBu)$ and $LiOC_6F_5$. However, based on the available data, we cannot completely rule out the possibility that $U(OC_6F_5)_5(THF)$ is also being formed. It is likely that in a coordinating solvent, such as THF, the solvation of $LiOC_6F_5$ is promoted, allowing ^{t}BuOH or THF to coordinate to uranium.

The isolation of **3** demonstrates the necessity of removing all LiI from samples of $U(O^tBu)_6$, and we have found that recrystallizing $U(O^tBu)_6$ from an Et_2O/MeCN mixture provides LiI-free product. With this material in hand, we reattempted the synthesis of $U(OC_6F_5)_6$ by alcoholysis. Addition of 6 equiv of freshly recrystallized C_6F_5OH to a solution of $U(O^tBu)_6$ in C_6D_6 quickly produces a deep-red solution. Upon standing, the reaction mixture bleaches to pale red-orange, concomitant with deposition of bright red needles. Analysis of this material by X-ray crystallography demonstrates the formation of a uranyl-containing product $UO_2(OC_6F_5)_2(HO^tBu)_2$ (**4**) and not $U(OC_6F_5)_6$ as anticipated (eq 4).

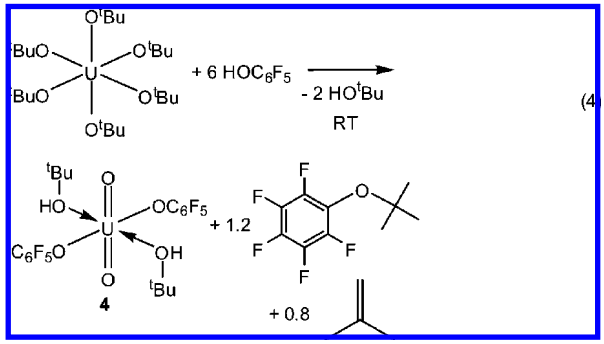

(4)

Complex **4** crystallizes in the monoclinic space group *C*2/*c*. Its solid-state molecular structure is shown in Figure 3. The metrical parameters of the uranyl moiety (U1−O1 = 1.771(6), O1−U1−O1* = 180°) in **4** are typical of UO_2^{2+}. The U−O(aryloxide) bond length in **4** (U1−O2 = 2.183(8) Å) is comparable to those observed in UO_2(O-2,6-^{i}Pr$_2$C$_6$H$_3$)$_2$(py)$_3$ (U−O = 2.179(5) Å, 2.215(5) Å) and $[Na(THF)_3]_2[UO_2$(O-2,6-^{i}Pr$_2$C$_6$H$_3$)$_4]$ (U−O = 2.217(5) Å, 2.190(5) Å). The U−O(*tert*-butanol) bond length (U1−O3 = 2.399(7) Å) is similar to those in other uranyl−alcohol adducts.[62] A handful of other uranyl aryloxides have been reported,[63,64] but they have not been structurally characterized.

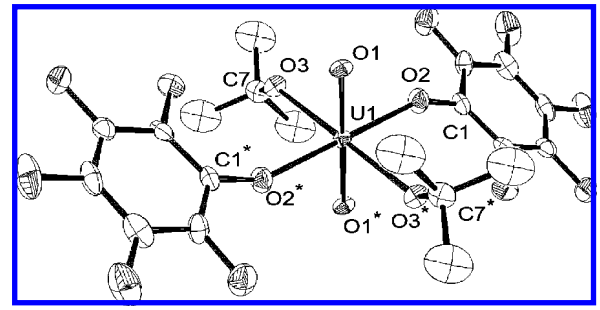

Figure 3. ORTEP diagram of $UO_2(OC_6F_5)_2(HO^tBu)_2$ (**4**) with 30% probability ellipsoids. Asterisks indicate symmetry-related atoms. Selected bond lengths (Å) and angles (deg): U1−O1 = 1.771(6), U1−O2 = 2.183(8), U1−O3 = 2.399(7), U1−O2−C1 = 153.8(7), U1−O3−C7 = 138.4(7), O1−U1−O2 = 88.0(3), O1−U1−O3 = 85.1(3), O2−U1−O3 = 89.9(3).

Complex **4** is insoluble in hexanes, sparingly soluble in arenes and CH_2Cl_2, and completely soluble in ethereal solvents, such as Et_2O and THF. The ^{1}H NMR spectrum of **4** in THF-d_8 consists of two resonances at 3.21 and 1.14 ppm in a 1:9 ratio, respectively. These signals are assignable to the hydroxyl and *tert*-butyl protons of the coordinated *tert*-butanol ligand, respectively. The ^{19}F{^{1}H} NMR spectrum displays resonances at −99.19, −103.89, and −114.04 ppm in a 2:2:1 ratio.

Monitoring the formation of **4** *in situ* in C_6D_6 by ^{1}H and ^{19}F{^{1}H} NMR spectroscopy reveals the formation of several other products in the reaction mixture. For instance, three new resonances at −89.77, −99.72, and −101.90 ppm in a 2:1:2 ratio are found in the ^{19}F{^{1}H} NMR spectrum, while a singlet is observed at 1.09 ppm in the ^{1}H NMR spectrum. We have assigned these resonances to ^{t}BuOC$_6$F$_5$ (eq 4).[65,66] Confirmation of this assignment was made by comparison of this spectrum to that of independently prepared ^{t}BuOC$_6$F$_5$,[67] and its presence was further established by GC/MS analysis. Also observed in the ^{1}H NMR spectrum are peaks at 1.60 ppm and 4.74 ppm in a 1:3 ratio, which we have assigned to isobutylene.[68] The presence of isobutylene was further confirmed by the ^{13}C{^{1}H} NMR spectrum, which exhibits resonances at 24.4, 111.4, and 142.4 ppm, closely matching those reported for the authentic material.[69] ^{t}BuOC$_6$F$_5$ and isobutylene were formed in a ratio of 1.2:0.8, as determined by integration of the resonances in the ^{1}H NMR spectrum.

Formation of an oxo group by elimination of isobutylene from a *tert*-butoxide ligand is well established,[68,70−73] while

(62) Storey, A. E.; Zonnevijlle, F.; Pinkerton, A. A.; Schwarzenbach, D. *Inorg. Chim. Acta* **1983**, *75*, 103–113.
(63) Funk, H.; Andrae, K. *Z. Anorg. Allg. Chem.* **1968**, *362*, 93–97.
(64) Malhotra, K. C.; Sharma, M.; Sharma, N. *Indian J. Chem.* **1985**, *24A*, 790–792.
(65) Bruce, M. I. *J. Chem. Soc. A* **1968**, 1459–1464.
(66) Pushkina, L. N.; Stepanov, A. P.; Zhukov, V. S.; Naumov, A. D. *Org. Magn. Reson.* **1972**, *4*, 607–623.
(67) Wakefield, B. J.; Cheong, C. L. *J. Chem. Soc., Perkin Trans. 1* **1988**, 3301–3305.
(68) Budzichowski, T. A.; Chisholm, M. H.; Strieb, W. E. *J. Am. Chem. Soc.* **1994**, *116*, 389–390.
(69) de Haan, J. W.; van de Ven, L. J. M.; Wilson, A. R. N.; van der Hout-Lodder, A. E.; Altona, C.; Faber, D. H. *Org. Magn. Reson.* **1976**, *8*, 477–482.
(70) Gibson, V. C.; Graham, A. J.; Ormsby, D. L.; Ward, B. P.; White, A. J. P.; Williams, D. J. *Dalton Trans.* **2002**, 2597–2598.

the formation of an oxo by elimination of ether is comparatively rare.[74−78] Nonetheless, there are a few examples of the C_6F_5 group participating in oxo formation. For instance, addition of 4 equiv of $NaOC_6F_5$ to $[Bi(OC_6F_5)_3(C_7H_8)]_2$ results in the isolation of a metal oxide, $Na_4Bi_2O(OC_6F_5)_8(THF)_4$, and formation of the diaryl ether, $C_6F_5OC_6F_5$.[78,79] In addition, aromatic nucleophilic substitution of electron-poor rings with strong nucleophiles is well documented.[67,80−83] Given this literature precedent, the formation of $^tBuOC_6F_5$ by a similar mechanism, i.e. intramolecular nucleophilic attack of the C_6F_5 ipso carbon by a *tert*-butoxide followed by C−O(aryloxide) bond cleavage, was deemed possible.

To test this mechanism, we prepared $C_6F_5{}^{18}OH$ by reaction of $K^{18}OH$ with C_6F_6 in DME. By this route we isolated $C_6F_5{}^{18}OH$ as a DME adduct, namely $C_6F_5{}^{18}OH\cdot0.5DME$, in moderate yields. The resulting product always contained approximately 0.5 equiv of DME regardless of the method of purification. C_6F_5OH is well known to form strong hydrogen-bonding interactions with Lewis bases, such as 1,4-dioxane and THF,[84−89] and we suspect that hydrogen bonding also occurs between DME and the $C_6F_5{}^{18}OH$ proton. Reaction of $U(O^tBu)_6$ with $C_6F_5{}^{18}OH\cdot0.5DME$ produces a deep-red reaction mixture. The deep color of the solution fades after 12 h, affording a red-orange solution concomitant with the deposition of $UO_2(OC_6F_5)_2(DME)$ (**5-^{18}O**) as an orange powder, which can be isolated in 55% yield (eq 5). Similarly, the unlabeled analogue (**5**) can be generated by addition of 6 equiv of $C_6F_5OH\cdot0.5DME$ to $U(O^tBu)_6$. Both the ^1H and $^{19}F\{^1H\}$ NMR spectra of **5-^{18}O** and **5** is consistent with the proposed formulations. For instance, the ^1H NMR spectrum of **5-^{18}O** in C_6D_6/THF-d_8 exhibits resonances attributable to coordinated DME at 3.15 and 3.31 ppm, while the $^{19}F\{^1H\}$ NMR spectrum exhibits resonances at −113.94, −105.21, and −102.32 ppm in a 1:2:2 ratio. In addition, both $^tBuOC_6F_5$ and isobutylene are still being generated during the formation of **5-^{18}O**, as determined by ^1H and $^{19}F\{^1H\}$ NMR spectroscopy, indicating that the overall course of the reaction has not changed despite the presence of DME.

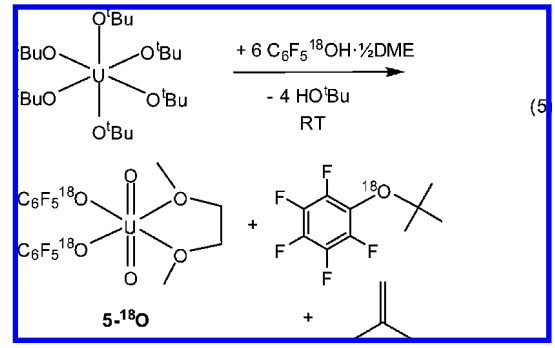

(5)

Examination of the volatile components of the reaction mixture by GC/MS revealed that the *tert*-butyl(pentafluorophenyl)ether generated during the course of the reaction contains the ^{18}O label (eq 5). Furthermore, the IR spectrum of **5-^{18}O**, as a KBr pellet, exhibits an absorption at 935 cm^{-1}, which is attributable to the U═O asymmetric stretch, and a peak at 1158 cm^{-1}, which is attributable to the C−O vibration of the pentafluorophenoxide ligand. The IR spectrum of **5** also exhibits an absorption at 935 cm^{-1} and a peak at 1179 cm^{-1}. This latter peak is shifted by the amount anticipated upon exchange of ^{18}O with ^{16}O. These results suggest that the oxygen in C_6F_5OH is not the source of the oxo ligands in either **4** or **5**, and that the oxo ligands solely the result of *tert*-butyl cation elimination. Based on these observations, we propose that an intermediate species, containing both *tert*-butoxide and pentafluorophenoxide ligands, is transiently generated by protonation of $U(O^tBu)_6$ with C_6F_5OH. This intermediate complex eliminates the *tert*-butyl cation, generating the uranyl fragment. The presence of $^tBuOC_6F_5$ is due to either the capture of the isobutylene by phenol, which is a known route for protecting an alcohol,[90] or the direct attack of the *tert*-butyl cation by a pentafluorophenoxide ligand. Interestingly, we see no evidence for the formation of di(*tert*-butylether) in the reaction mixture, probably for steric reasons.[91]

Several other products were also present during the formation of **4**, as revealed by $^{19}F\{^1H\}$ NMR spectroscopy. At short reaction times, these species are observed in relatively high concentrations, but as the reaction proceeds their ^{19}F resonances diminish in intensity while the peaks associated with **4** and $^tBuOC_6F_5$ increase in intensity. We have endeavored to isolate these intermediate species generated during the formation of **4**. In one attempt, excess C_6F_5OH was added to $U(O^tBu)_6$ in pentane, and rapid cooling of this solution to −25 °C provided a few dark crystals of a

(71) Mayer, J. M. *Polyhedron* **1995**, *14*, 3273–3292.
(72) Nobel, A. M.; Winfield, J. M. *J. Chem. Soc. A* **1970**, 501–506.
(73) Fandos, R.; Hernandez, A. O.; Rodriguez, A.; Ruiz, M. J.; Terreros, P. *Dalton Trans.* **2002**, 11–13.
(74) Turova, N. Y.; Kessler, V. G.; Kucheiko, S. I. *Polyhedron* **1991**, *10*, 2617–2628.
(75) Turova, N. Y.; Kessler, V. G.; Mironov, A. V. *Polyhedron* **1993**, *12*, 1573–1576.
(76) Kessler, V. G.; Shevelkov, A. V.; Bengtsson-Kloo, L. A. *Polyhedron* **1998**, *17*, 965–968.
(77) Turova, N. Y.; Turevskaya, E. P.; Kessler, V. G.; Yanovskaya, M. I. *The Chemistry of Metal Alkoxides*; Kluwer Academic Publishers: Boston, MA, 2002.
(78) Jolas, J. L.; Hoppe, S.; Whitmire, K. H. *Inorg. Chem.* **1997**, *36*, 3335–3340.
(79) Whitmire, K. H.; Jones, C. M.; Burkart, M. D.; Hutchison, J. C.; McKnight, A. L. *Mater. Res. Soc. Symp. Proc.* **1992**, *271*, 149–154.
(80) Chambers, R. D.; Musgrave, K. R.; Waterhouse, J. S.; Williams, D. L. H.; Burdon, J.; Hollyhead, W. B.; Tatlow, J. C. *Chem. Commun.* **1974**, 239–240.
(81) Bolton, R.; Sandall, J. P. B. *J. Chem. Soc., Perkin Trans. 2* **1976**, 1541–1545.
(82) Chambers, R. D.; Close, D.; Williams, D. L. H. *J. Chem. Soc., Perkin Trans. 2* **1980**, 778–780.
(83) Chambers, R. D.; Seabury, M. J.; Williams, D. L. H. *J. Chem. Soc., Perkin Trans. 1* **1988**, 255–257.
(84) Birknes, B. *Acta Chem. Scand. B* **1976**, *30*, 450–454.
(85) Domasevitch, K. *Acta Crystallogr., Sect. C* **2008**, *C64*, 326–329.
(86) Gramstad, T.; Husebye, S.; Maartmann-Moe, K. *Acta Chem. Scand. B* **1985**, *39*, 767–771.
(87) Wolff, H.; Zeller, W. *J. Phys. Chem.* **1982**, *86*, 5243–5247.
(88) Kuopio, R. *Acta Chem. Scand. A* **1977**, *31*, 369–374.
(89) Gramstad, T.; Husebye, S.; Maartmann-Moe, K.; Saebo, J. *Acta Chem. Scand. B* **1987**, *41*, 555–563.
(90) Greene, T. W.; Wuts, P. G. M. *Protective Groups in Organic Synthesis*, 3rd ed.; John Wiley & Sons, Inc.: New York, 1999.
(91) Smutny, E. J.; Bondi, A. *J. Phys. Chem.* **1961**, *65*, 546–550.

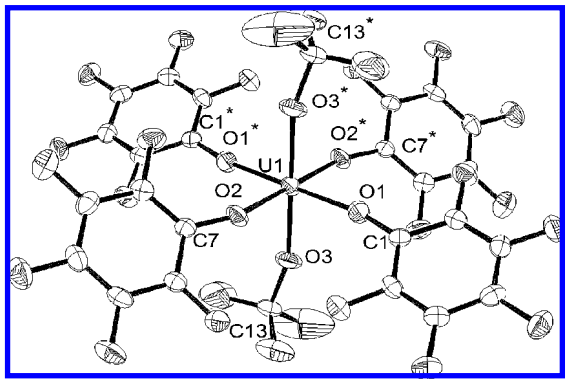

Figure 4. ORTEP diagram of $U(O^tBu)_2(OC_6F_5)_4$ (**6**) with 30% probability ellipsoids. Asterisks indicate symmetry-related atoms. Selected bond lengths (Å), and angles (deg): U1−O1 = 2.104(7), U1−O2 = 2.091(6), U1−O3 = 2.148(7), U1−O1−C1 = 170.1(6), U1−O2−C7 = 156.4(6), U1−O3−C13 = 159.9(8), O1−U1−O2 = 90.5(3), O1−U1−O3 = 90.2(3), O2−U1−O3 = 90.4(3).

new complex. X-ray crystallographic analysis of this material revealed the formation of a mixed alkoxy-aryloxide $U(O^tBu)_2(OC_6F_5)_4$ (**6**) (eq 6).

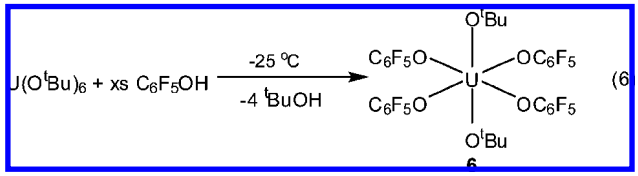

(6)

Complex **6** crystallizes in the triclinic space group $P\bar{1}$, and its solid-state molecular structure is shown in Figure 4. Complex **6** exhibits an octahedral geometry with a trans arrangement of its two *tert*-butoxide ligands. The U−O bond lengths in **6** (U1−O1 = 2.104(7) Å, U1−O2 = 2.091(6) Å, and U1−O3 = 2.148(7) Å) is comparable to those found in $U(OCH_3)_6$[25] and $U(O^tBu)_6$,[28] as are the U−O−C bond angles (U1−O1−C1 = 170.1(6)°, U1−O2−C7 = 156.4(6)°, and U1−O3−C13 = 159.9(8)°). Interestingly, the *tert*-butoxide and phenoxide U−O bonds lengths are identical by the 3σ criterion. This is surprising, considering that alkoxide ligands generally considered stronger π-donors than are aryloxides.[24,51]

It is likely that the formation of **4** proceeds via complex **6**, but attempts to isolate **6** on larger scales to further probe its intermediacy in the reaction have not been successful. Our inability to isolate this molecule reproducibly may be a result of its ability to easily eliminate the *tert*-butyl cation. Complex **6** is anticipated to be relatively electron poor and to compensate for the loss of the strongly electron-donating *tert*-butoxide ligand, it may eliminate the *tert*-butyl cation (concomitant with the formation of an oxo). This reasoning is supported by the electrochemical properties of **1** and **2**, which clearly demonstrate that the U(VI) center becomes electron deficient as *tert*-butoxide ligands are exchanged. No doubt the formation of the strong U═O bonds of the uranyl moiety, which has a large bond enthalpy, also plays a role.[21] The formation of **4** also occurs when only 4 equiv of C_6F_5OH is added to solutions of $U(O^tBu)_6$, which provides further support that complex **6** is the intermediate that undergoes *tert*-butyl cation elimination. Not surprisingly, the addition of 2 equiv of C_6F_5OH to **2** also results in the isolation of **4**.

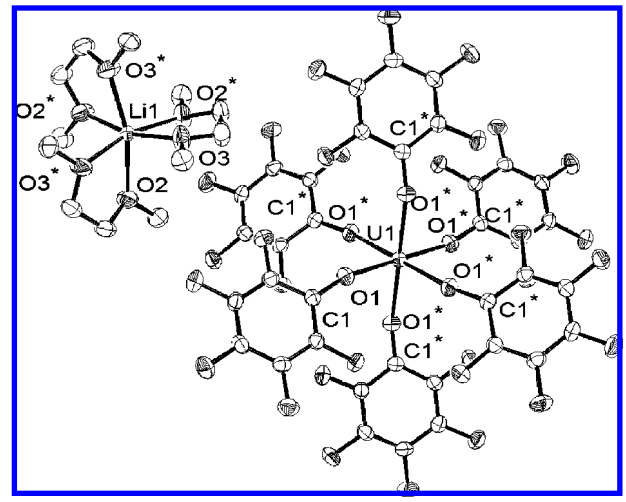

Figure 5. ORTEP diagram of $[Li(DME)_3]_2[U(OC_6F_5)_6]$ (**7**) with 30% probability ellipsoids and one $[Li(DME)_3]$ cation depicted. Asterisks indicate symmetry-related atoms. Selected bond lengths (Å) and angles (deg): U1−O1 = 2.218(2), Li1−O2 = 2.151(6), Li1−O3 = 2.112(6), U1−O1−C1 = 160.7(2), O2−Li1−O3 = 97.9(1).

To circumvent the formation of **4**, we attempted to synthesize a butoxide-free precursor, namely the uranium(IV) homoleptic aryloxide $[U(OC_6F_5)_6]^{2-}$, which could then be oxidized by $2e^-$ to provide the target U^{6+} complex. Thus, addition of 10 equiv of C_6F_5OH to $[Li(THF)]_2[U(O^tBu)_6]$ in Et_2O results in the formation of a green-amber solution. Removal of the solvent in vacuo and recrystallization of the resulting oil from a Et_2O/DME/hexanes mixture provides pale-pink blocks of $[Li(DME)_3]_2[U(OC_6F_5)_6]$ (**7**) in 81% yield (eq 7).

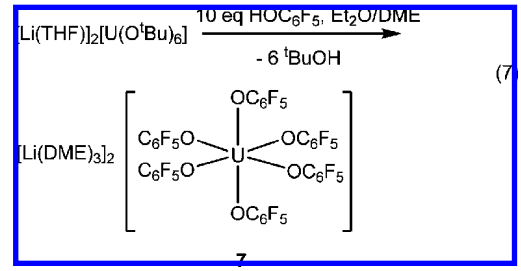

(7)

The ^1H NMR spectrum of **7** in CD_2Cl_2 displays two broad resonances attributable to the coordinated DME at 3.02 and 2.42 ppm, while the $^{19}F\{^1H\}$ NMR spectrum of **7** in CD_2Cl_2 consists of three broad signals at −105.22, −107.84, and −111.50 ppm in a 2:2:1 ratio. The $^7Li\{^1H\}$ NMR spectrum contains a broad singlet at −22.55 ppm. Complex **7** is insoluble in hexanes, partly soluble in arenes, and soluble in Et_2O or THF. Interestingly, despite containing DME, **7** is completely insoluble in that solvent.

Complex **7** crystallizes in the rhombohedral space group $R\bar{3}$, and its solid-state molecular structure is shown in Figure 5. The octahedral uranium center in **7** is coordinated by six pentafluorophenoxide ligands, and in contrast to complex **3**, the lithium cations do not interact with the aryloxide oxygen atoms. Instead each lithium is coordinated by three DME molecules resulting in a distorted octahedral geometry about Li (O2−Li1−O3 = 97.9(1)°). The U−O bond length (U1−O1 = 2.218(2) Å) and U−O−C(ipso) bond angle

Scheme 1

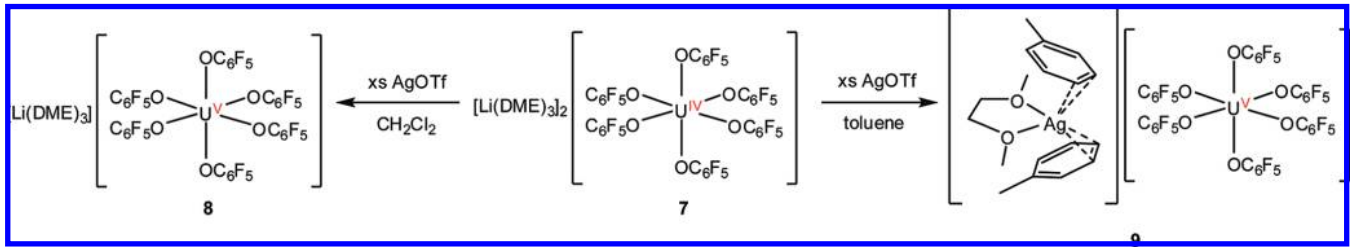

(U1−O1−C1 = 160.7(2)°) are comparable to those of other U(VI) aryloxides.[92−95]

The electrochemical properties of **7** were investigated by cyclic voltammetry. The cyclic voltammogram of **7** in CH_2Cl_2 displays a seemingly reversible oxidation feature at −0.38 V (vs $[Cp_2Fe]^{0/+}$) (see Supporting Information), which we have assigned to the U(V)/U(IV) redox couple. This feature exhibits large peak separation between the cathodic and anodic waves (ΔE_p = 435 mV at 200 mV·s^{-1}), suggesting poor electron-transfer kinetics.[96] A small shoulder centered at 0.18 V (at a scan rate of 1.0 V/s) was observed next to the anodic wave, which we have not been able to assign. This shoulder becomes more pronounced with increasing scan rate. In addition, the cyclic voltammogram of **7** also exhibits a reduction feature at $E_{1/2}$ = −1.51 V (vs $[Cp_2Fe]^{0/+}$), which we have assigned to the U(IV)/U(III) redox couple. However, this feature is broad and the peak separation between the cathodic and anodic waves is large (ΔE_p = 530 mV at 200 mV·s^{-1}). Notably absent from the cyclic voltammogram of **7** (within the range of the solvent window) is the presence of any oxidation feature attributable to a U(V)/U(VI) redox couple.

Further support for our assignment of the oxidation feature at −0.38 V comes from the oxidation of **7** by chemical means. Thus, the addition of 2 equiv of AgOTf to **7** in CH_2Cl_2 or toluene provides $[Li(DME)_3][U(OC_6F_5)_6]$ (**8**) or $[Ag(\eta^2\text{-}C_7H_8)_2(DME)][U(OC_6F_5)_6]$ (**9**), respectively (Scheme 1).

The ^{1}H NMR spectrum of **8** in CD_2Cl_2 consists of two resonances at 3.60 and 3.43 ppm which we have assigned to coordinated DME. The ^{7}Li{^{1}H} NMR spectrum of **8** in CD_2Cl_2 exhibits a singlet at −1.90 ppm, and the ^{19}F{^{1}H} NMR spectrum exhibits three resonances at −99.03, −104.16, and −105.19 ppm in a 2:2:1 ratio, respectively. The ^{1}H NMR spectrum of **9** displays resonances attributable to DME at 3.62 and 3.45 ppm, and resonances corresponding to toluene at 7.30, 7.25, 7.19, and 2.37 ppm. Consistent with its solid-state molecular structure (vide infra), no signal was observed in the ^{7}Li{^{1}H} NMR spectrum of **9**. The ^{19}F{^{1}H} NMR spectrum of **9** is similar to that observed for **8**. Notably, when **8** and **9** are dissolved in CD_2Cl_2 we have never observed any disproportionation or decomposition. We have also recorded the UV−vis/NIR spectrum of complex **9** (see Supporting Information). The spectrum is qualitatively similar to those observed for $[UX_6]^-$ (X = Cl, Br)[97] and provides further evidence for the 5f^1 electronic configuration.

Single crystals of **9** suitable for X-ray crystallographic analysis were grown from a toluene/hexanes mixture. Complex **9** crystallizes in the triclinic space group $P\bar{1}$, and contains two independent uranium centers within the asymmetric unit, each positioned on a crystallographic inversion center. The solid-state molecular structure of one full molecule, generated by symmetry along with the silver-containing counterion, is shown in Figure 6.

The uranium center in **9** exhibits a distorted octahedral geometry (O4−U2−O4* = 180°, O4−U2−O5 = 91.0(2)°, and O4−U2−O6 = 92.0(2)°). Its U−O bond lengths (U2−O4 = 2.114(5) Å, U2−O5 = 2.102(5) Å, and U2−O6 = 2.110(4) Å) are approximately 0.1 Å shorter than those observed in **7** (U1−O1 = 2.218(2) Å), which is consistent with the presence of the smaller U^{5+} ion.[98] Not surprisingly, the U−O bond lengths of **9** are comparable to the U−O(terminal) bond lengths in **3**. The U−O−C(ipso) bond angles in **9** are U2−O5−C25 = 157.3(5)°, U2−O6−C31 = 161.4(4)°, and U2−O4−C19 = 146.8(4)°. In addition, each pentafluorophenoxide ligand participates in $\pi-\pi$ interactions with the pentafluorophenoxide rings of the neighboring complexes in the crystal lattice (see Supporting

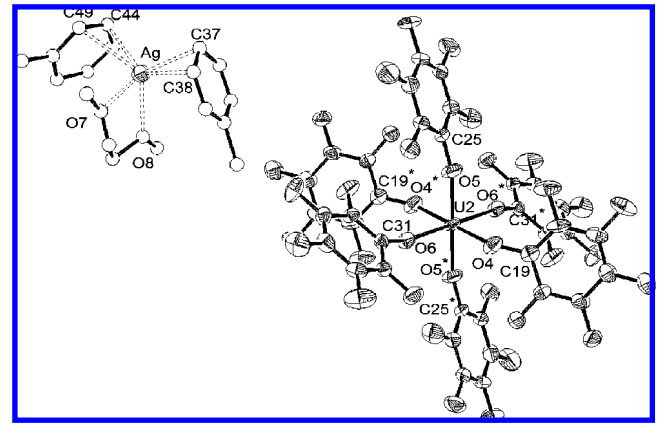

Figure 6. ORTEP diagram of $[Ag(\eta^2\text{-}C_7H_8)_2(DME)][U(OC_6F_5)_6]$ (**9**) with 30% probability ellipsoids and one of two uranium centers shown. Asterisks indicate symmetry-related atoms. Selected bond lengths (Å) and angles (deg): U2−O4 = 2.114(5), U2−O5 = 2.102(5), U2−O6 = 2.110(4), Ag−C37 = 2.452(9), Ag−C38 = 2.73(1), Ag−C44 = 2.49(1), Ag−C49 = 2.732(9), Ag−O7 = 2.37(1), Ag−O8 = 2.353(5), U2−O4−C19 = 146.8(4), U2−O5−C25 = 157.3(5), U2−O6−C31 = 161.4(4), O4−U2−O5 = 91.0(2), O4−U2−O6 = 92.0(2).

(92) Lappert, M. F.; Blake, P. C.; Taylor, R. G. *Inorg. Chim. Acta* **1987**, *139*, 303–315.
(93) Van Der Sluys, W. G.; Sattelberger, A. P. *Polyhedron* **1989**, *8*, 1247–1249.
(94) Clark, D. L.; Berg, J. M.; Huffman, J. C.; Morris, D. E.; Sattelberger, A. P.; Streib, W. E.; Van Der Sluys, W. G.; Watkin, J. G. *J. Am. Chem. Soc.* **1992**, *114*, 10811–10821.
(95) Clark, D. L.; Sattelberger, A. P.; Van Der Sluys, W. G. *J. Alloys Compd.* **1992**, *180*, 303–315.
(96) Morris, D. E. *Inorg. Chem.* **2002**, *41*, 3542–3547.

Information). This may be the cause of the relatively acute U2−O4−C19 angle. The silver cation in **9** is ligated by two toluene molecules, each coordinated in an η^2 fashion, and one DME molecule. The ligation of Ag^+ by arenes is well documented.[99−103] The Ag−C bond distances in **9** are Ag−C37 = 2.452(9), Ag−C38 = 2.73(1), Ag−C44 = 2.49(1), and Ag−C49 = 2.732(9) Å, while the Ag−O bond lengths are 2.37(1) and 2.353(5) Å. The Ag−C distances are within the range of other known η^2-arene interactions.[100−103] In addition, the solid-state molecular structure of **9** also reveals $\pi-\pi$ interactions between the silver-bound toluene molecule and a pentafluorophenoxide ring (see Supporting Information). The presence of silver in complex **9** is likely due to the use of excess AgOTf in the reaction. The exchange of lithium for silver using AgX (X = OTf, BF_4) is well known and is no doubt facilitated by use of toluene as the solvent.[103,104]

Solvent can also have a considerable effect on the oxidation potential of Ag^+.[61] However, in neither CH_2Cl_2 nor toluene was there any evidence for the formation of a U(VI) complex. Thus, we attempted the oxidation of **8** with a much stronger oxidant, specifically [NO][BF_4] ($E° = 1.00$ V vs $[Cp_2Fe]^{0/+}$).[61] The reaction of 1 equiv of [NO][BF_4] with **8** in CD_2Cl_2 was monitored by $^{19}F\{^1H\}$ NMR spectroscopy. The reaction between **8** and [NO][BF_4] is slow, but over the course of several days the signals attributable to **8** slowly decrease in intensity, while a plethora of new resonances appear. The only tractable material that could be isolated from the reaction mixtures were small amounts of the starting material. The reaction of [NO][BF_4] with C_6F_5OH in CD_2Cl_2 was also monitored by $^{19}F\{^1H\}$ NMR spectroscopy. This also results in the formation of many products, as indicated by the $^{19}F\{^1H\}$ NMR spectrum. Interestingly, many of the signals observed in this spectrum also matched those observed upon oxidation of **8**. The close similarity between the two sets of spectra suggests that the oxidation of **8** by [NO][BF_4] is largely ligand based. Indeed, the oxidation of pentafluorophenol in known to generate a complex mixture of products in solution.[105,106] In our case, it is possible that the oxidation of **8** with [NO][BF_4] transiently generates $U(OC_6F_5)_6$, but the inability to isolate this complex suggests that the pentafluorophenoxide ligand cannot support the U^{6+} oxidation state, and it subsequently decomposes via ligand oxidation.

A comparison of the metrical parameters of complexes **3** and **9** with those reported for the related tungsten(V) aryloxides is potentially informative. Both $[Li(THF)_2][W(OC_6H_5)_6]$ and $[NEt_4][W(OC_6H_5)]$ have been structurally characterized.[107] As anticipated, the W−O(terminal) bond lengths in $[Li(THF)_2][W(OC_6H_5)_6]$ (av 1.918 Å) and $[NEt_4][W(OC_6H_5)]$ (av 1.943 Å) are smaller than U−O(terminal) bonds in **3** (av 2.088 Å) and **9** (av 2.109 Å). This difference is similar to the difference in ionic radii between W(V) (0.76 Å for CN = 6) and U(V) (0.90 Å for CN = 6).[98] However, the terminal W−O−C(ipso) bond angles in $[Li(THF)_2][W(OPh)_6]$ (av 139.9°) and $[NEt_4][W(OC_6H_5)_6]$ (av 139.0°) are considerably smaller than the U−O−C angles observed in **3** (av 165.3°) and **9** (av 155.2(4)°. This difference may arise because uranium possesses orbital combinations that are not possible for the Group 6 metals, and any increased π-donation from the oxygen lone pairs would result in larger U−O−C angles.[25] However, the larger average U−O−C angles in **3** and **9** do not seem to impart an enhanced stability of the 6+ oxidation state, as we could not access the target complex, $U(OC_6F_5)_6$, by chemical or electrochemical means. If molecules of this type are isolated, then our preliminary results suggest that they would be potent oxidants. In contrast, many tungsten(VI) aryloxides are known,[108−111] including $W(OC_6F_5)_6$,[112] which can be synthesized by protonation of WCl_6 with HOC_6F_5. Taken together, these results demonstrate the limits of π-bonding in uranium to stabilize higher oxidation states and highlight the care required in choosing uranium coligands.

Summary

The isolation of $U(O^tBu)_5(OC_6F_5)$, $U(O^tBu)_4(OC_6F_5)_2$, and $U(O^tBu)_2(OC_6F_5)_4$ demonstrates the feasibility of coordinating aryloxides to a uranium(VI) center. As shown by the reduction potentials of $U(O^tBu)_5(OC_6F_5)$ and $U(O^tBu)_4(OC_6F_5)_2$, the pentafluorophenoxide ligand is not as capable of stabilizing the 6+ oxidation state as is the *tert*-butoxide ligand. We interpret the increase in reduction potential as a manifestation of the decreased capacity of the aryloxide oxygen to contribute electron density by π-donation to the metal, which we believe argues for a substantial π-contribution to the overall metal−ligand bonding framework. Attempts to isolate the complete *tert*-butoxide/pentafluorophenoxide series were hampered by the formation of the uranyl complex, $UO_2(OC_6F_5)_6(HO^tBu)_2$. This complex arises via elimination of a *tert*-butyl cation from a *tert*-butoxide group, resulting in the formation of an oxo moiety, isobutylene, and $^tBuOC_6F_5$. We also endeavored to isolate $U(OC_6F_5)_6$ by first synthesizing the homoleptic uranium(IV) complex [Li-

(97) Ryan, J. L. *J. Inorg. Nucl. Chem.* **1971**, *33*, 153–177.
(98) Shannon, R. D. *Acta Crystallogr., Sect. A* **1976**, *32*, 751–767.
(99) Taylor, I. F.; Amma, E. L. *Chem. Commun.* **1970**, 1442–1443.
(100) Hall Griffith, E. A.; Amma, E. L. *J. Am. Chem. Soc.* **1971**, *93*, 3167–3172.
(101) Munakata, M.; Wu, L. P.; Ning, G. L.; Kuroda-Sowa, T.; Maekawa, M.; Suenaga, Y.; Maeno, N. *J. Am. Chem. Soc.* **1999**, *121*, 4968–4976.
(102) Elliot, E. L.; Hernandez, G. A.; Linden, A.; Siegel, J. S. *Org. Biomol. Chem.* **2005**, *3*, 407–413.
(103) Krossing, I. *Chem. Eur. J.* **2001**, *7*, 490–502.
(104) Krossing, I.; Trapp, N.; Reisinger, A. *Organometallics* **2007**, *26*, 2096–2105.
(105) Devynck, J.; Hadid, A. B.; Virelizier, H. *J. Fluorine Chem.* **1979**, *14*, 363–372.
(106) Fang, X.; Schuchmann, H.-P.; von Sonntag, C. *J. Chem. Soc., Perkin Trans. 2* **2000**, 1391–1398.
(107) Davies, J. I.; Gibson, J. F.; Skapski, A. C.; Wilkinson, G.; Wong, W.-K. *Polyhedron* **1982**, *1*, 641–646.
(108) Cross, W. B.; Parkin, I. P.; O'Neill, S. A.; Williams, P. A.; Mahon, M. F.; Molloy, K. C. *Chem. Mater.* **2003**, *15*, 2786–2796.
(109) Handy, L. B.; Benham, C.; Brinckman, F. E.; Johannesen, R. B. *J. Fluorine Chem.* **1976**, *8*, 55–67.
(110) Mortimer, P. I.; Strong, M. I. *Aust. J. Chem.* **1965**, *18*, 1579–1587.
(111) Sydora, O. L.; Goldsmith, J. I.; Vaid, T. P.; Miller, A. E.; Wolczanski, P. T.; Abruña, H. D. *Polyhedron* **2004**, *23*, 2841–2856.
(112) Beck, W.; Stetter, K. H.; Tadros, S.; Schwarzhans, K. E. *Chem. Ber.* **1967**, *100*, 3944–3954.

$(DME)_3]_2[U(OC_6F_5)_6]$. However, oxidation of $[Li(DME)_3]_2$-$[U(OC_6F_5)_6]$ by 2 equiv of AgOTf only produces uranium(V)-containing materials. Reaction of $[Li(DME)_3][U(OC_6F_5)_6]$ with the strong oxidant, $[NO][BF_4]$, in CH_2Cl_2 also does not result in the isolation of a U(VI) complex. Instead, the products generated appear to arise from oxidation of the pentafluorophenoxide ligand. Thus it appears that the pentafluorophenoxide group is incapable of stabilizing a homoleptic uranium(VI) aryloxide. In this regard, we will continue to study the coordination of uranium(VI) with other aryloxide ligands in an effort to synthesize $U(OAr)_6$ and gain further insight into the chemistry and bonding of uranium(VI).

Experimental Section

General. All reactions and subsequent manipulations were performed under anaerobic and anhydrous conditions and either under a high vacuum or an atmosphere of argon or nitrogen. Diethyl ether, toluene, hexanes, and THF were dried using a Vacuum Atmospheres DRI-SOLV solvent purification system. DME was distilled from sodium benzophenone ketyl. All deuterated solvents were purchased from Cambridge Isotope Laboratories Inc. and were dried over activated 4 Å molecular sieves for 24 h prior to use. CH_2Cl_2 and MeCN were stored under inert atmosphere over activated 3 Å molecular sieves for 24 h prior to use. C_6F_5OH (99+%) was purchased from Sigma Aldrich and recrystallized from hexanes. $[Li(THF)]_2[U(O^tBu)_6]$,[28] $U(O^tBu)_6$,[28] and $^tBuOC_6F_5$[67] were synthesized according to the published procedures. All other reagents were obtained from commercial sources and used as received.

NMR spectra were recorded on a Varian UNITY INOVA 400 or a Varian UNITY INOVA 500 spectrometer. ^1H and $^{13}C\{^1H\}$ NMR spectra were referenced to external $SiMe_4$ using the residual protio solvent peaks as internal standards (^1H NMR experiments) or the characteristic resonances of the solvent nuclei (^{13}C NMR experiments). $^7Li\{^1H\}$ NMR spectra were referenced to an external saturated solution of LiCl in deuterium oxide. $^{19}F\{^1H\}$ NMR spectra were referenced to external α,α,α-trifluorotoluene. Elemental analyses were performed by the Micro-Mass Facility at the University of California, Berkeley. IR spectra were recorded on a Mattson Genesis FTIR spectrometer while UV−vis/NIR spectra were recorded on a UV-3600 Shimadzu spectrophotometer. Mass spectra were recorded using a VG70 mass spectrometer at an ionizing voltage of 70 eV, and GC/MS analyses were performed using a Hewlett-Packard 5970B GC/MSD at an ionizing voltage of 70 eV.

Cyclic Voltammetry Measurements. CV experiments were performed using a CH Instruments 600c potentiostat, and the data were processed using CHI software (version 6.29). All experiments were performed in a glovebox using a 20 mL glass vial as the cell. The working electrode was a platinum disk embedded in glass (2 mm diameter), the counter electrode was a platinum wire, and the reference electrode was AgCl plated on Ag wire. Solutions employed during CV studies were typically 3 mM in the uranium complex and 0.1 M in $[Bu_4N][PF_6]$. All potentials are reported versus the $[Cp_2Fe]^{0/+}$ couple. For all trials, $i_{p,a}/i_{p,c} = 1$ for the $[Cp_2Fe]^{0/+}$ couple, while $i_{p,c}$ increased linearly with the square root of the scan rate (i.e., $\sqrt{\nu}$). Redox couples which exhibited behavior similar to the $[Cp_2Fe]^{0/+}$ couple were, thus, considered reversible.

$U(O^tBu)_5(OC_6F_5)$ (1). To a stirring solution of $U(O^tBu)_6$ (0.100 g, 0.148 mmol) in hexanes (4 mL) was added C_6F_5OH (0.027 g, 0.148 mmol) dissolved in hexanes (1 mL). The resulting solution immediately turned dark-red. After 4 days, the solvent was removed in vacuo. The dark-red solid was dissolved in diethyl ether (2 mL) and the solution was layered onto MeCN (10 mL) and stored at −25 °C for 24 h. This resulted in the deposition of dark-red crystals, which were collected and dried under vacuum: 0.082 g, 70% yield. ^1H NMR (500 MHz, 22 °C, C_6D_6): δ 1.58 (s, 9H, CCH_3), 1.60 (s, 36H, CCH_3). $^{13}C\{^1H\}$ (125 MHz, 22 °C, C_6D_6): δ 35.43 (CCH_3), 36.84 (CCH_3), 93.45 (CCH_3), 97.65 (CCH_3). $^{19}F\{^1H\}$ (376 MHz, 22 °C, C_6D_6): δ −112.17 (triplet of triplets, 1F, $^3J_{FF} = 22.8$ Hz, $^4J_{FF} = 7.5$ Hz, *p*-F), −106.10 (t, 2F, $^3J_{FF} = 22.7$ Hz, *m*-F), −97.65 (d, 2F, $^3J_{FF} = 19.3$ Hz, *o*-F). Anal. Calcd for $C_{26}H_{45}F_5O_6U$: C, 39.69; H, 5.77. Found: C, 39.64; H, 5.74.

$U(O^tBu)_4(OC_6F_5)_2$ (2). To a stirring solution of $U(O^tBu)_6$ (0.099 g, 0.146 mmol) in hexanes (4 mL) was added C_6F_5OH (0.054 g, 0.292 mmol) dissolved in hexanes (1 mL). The resulting solution immediately turned dark-red. After 4 h of stirring, the solvent was removed in vacuo, and the resulting dark-red solid was dissolved in diethyl ether (2 mL). This solution was layered onto MeCN (7 mL) and stored at −25 °C for 12 h. This resulted in the deposition of dark-red crystals, which were collected and dried under vacuum: 0.085 g, 65% yield. ^1H NMR (500 MHz, 22 °C, C_6D_6): δ 1.52 (s, 18H, CCH_3 *cis* isomer), 1.57 (s, 36H, CCH_3 *trans* isomer), 1.58 (s, 18H, CCH_3 *cis* isomer), *cis* and *trans* isomers were observed in a 1:4 ratio. $^{13}C\{^1H\}$ (125 MHz, 22 °C, C_6D_6): δ 32.31 (CCH_3 *cis* isomer), 34.74 (CCH_3 *trans* isomer), 36.35 (CCH_3 *cis* isomer), 103.65 (CCH_3 *trans* isomer), *cis* CCH_3 not observed. $^{19}F\{^1H\}$ (376 MHz, 22 °C, C_6D_6): δ −109.42 (triplet of triplets, 2F, $^3J_{FF} = 22.8$ Hz, $^4J_{FF} = 6.6$ Hz, *p*-F *trans* isomer), −108.05 (triplet of triplets, 2F, $^3J_{FF} = 22.8$ Hz, $^4J_{FF} = 5.9$ Hz, *p*-F *cis* isomer), −105.11 (t, 4F, $^3J_{FF} = 21.4$ Hz, *m*-F *cis* isomer), −104.84 (t, 4F, $^3J_{FF} = 20.9$ Hz, *m*-F *trans* isomer), −98.21 (dd, 4F, $^3J_{FF} = 19.2$, $^4J_{FF} = 6.6$ Hz, *o*-F *trans* isomer), −97.54 (d, 4F, $^3J_{FF} = 22.0$ Hz, *o*-F *cis* isomer). Anal. Calcd for $C_{28}H_{36}F_{10}O_6U$: C, 37.50; H, 4.05. Found: C, 37.48; H, 4.22.

$[Li(HO^tBu)_2][U(OC_6F_5)_6]$ (3). To a stirring solution of $U(O^tBu)_6$ (0.061 g, 0.090 mmol) in toluene (2 mL) was added LiI (0.012 g, 0.090 mmol). A solution of C_6F_5OH (0.099 g, 0.540 mmol) in toluene (1 mL) was then added dropwise. The dark-red solution was stirred for 6 h. Removal of the solvent in vacuo yielded a dark red solid, which was rinsed with hexanes (2 mL) and dried under vacuum: 0.075 g, 56% yield. ^1H NMR (400 MHz, 22 °C, CD_2Cl_2): δ 0.95 (s, 18H, Me), 1.57 (br s, 2H, OH). $^7Li\{^1H\}$ NMR (194 MHz, 22 °C, CD_2Cl_2): δ 0.94 (s). $^{19}F\{^1H\}$ (376 MHz, 22 °C, CD_2Cl_2): δ −105.00 (s), −102.89 (s), −102.61 (br s), −102.28 (s), −101.78 (s), −100.88 (s), −100.37 (s), −99.73 (br s), −99.23 (s). $^7Li\{^1H\}$ NMR (194 MHz, 22 °C, CD_2Cl_2/DME): δ −2.68 (s). $^{19}F\{^1H\}$ NMR (376 MHz, 22 °C, CD_2Cl_2/DME): δ −99.67 (s, 12F, *o*-F), −105.44 (s, 12F, *m*-F), −108.88 (s, 6F, *p*-F). ^1H NMR (500 MHz, 22 °C, THF-d_8): δ 1.15 (s, 18H, CCH_3), OH not observed. $^7Li\{^1H\}$ NMR (194 MHz, 22 °C, THF-d_8): δ 0.34 (s). $^{19}F\{^1H\}$ NMR (470 MHz, 22 °C, THF-d_8): δ −97.99 (s, 12F, *o*-F), −104.40 (s, 12F, *m*-F), −108.19 (s, 6F, *p*-F). Anal. Calcd for $C_{44}H_{20}F_{30}LiO_8U$: C, 35.43; H, 1.35. Found: C, 35.59; H, 1.71.

$UO_2(OC_6F_5)_2(HO^tBu)_2$ (4). To a solution of $U(O^tBu)_6$ (0.046 g, 0.068 mmol) in hexanes (4 mL) was added C_6F_5OH (0.080 g, 0.435 mmol) dissolved in hexanes (1 mL). The resulting dark-red solution gradually lightened over the course of 3.5 h, affording a red-orange solution concomitant with the deposition of bright-red needles. The supernatant was decanted, and the crystals were washed with hexanes (2 × 2 mL) and dried under vacuum: 0.027 g, 51% yield. ^1H NMR (500 MHz, 22 °C, THF-d_8): δ 1.14 (s, 18H, CCH_3), 3.21 (s, 2H, OH). $^{19}F\{^1H\}$ NMR (470 MHz, 22 °C, THF-d_8): δ −114.04 (m, 2F, $J_{FF} = 10.4$ Hz, *p*-F), −103.89 (t, 4F, $^3J_{FF} = 20.2$ Hz, *m*-F), −99.19 (dd, 4F, $^3J_{FF} = 18.6$ Hz, $^4J_{FF} = 7.3$ Hz,

o-F). $^{13}C\{^1H\}$ (125 MHz, 22 °C, C_6D_6/THF-d_8): δ 31.68 (CCH_3). IR (KBr pellet, cm^{-1}): 3370 (w), 2985 (w), 1651 (w), 1631 (w), 1518 (s), 1479 (s), 1378 (m), 1315 (m), 1249 (w), 1172 (s), 1022 (s), 995 (s), 896 (s, ν_{asym} U=O), 854 (m), 739 (m), 651 (m), 479 (m). Anal. Calcd for $C_{20}H_{20}F_{10}O_6U$: C, 30.62; H, 2.58. Found: C, 30.26; H, 2.35.

$UO_2(OC_6F_5)_2(DME)$ (5). To a vial containing C_6F_5OH (0.084 g, 0.456 mmol) and DME (0.024 mL) was added $U(O^tBu)_6$ (0.042 g, 0.062 mmol) dissolved in hexanes (5 mL). The resulting dark-red solution gradually lightened over the course of 12 h, affording a red-orange solution concomitant with the deposition of an orange powder. The supernatant was decanted off, and the powder was washed with hexanes (2 × 2 mL) and dried under vacuum: 0.023 g, 51% yield. ^1H NMR (500 MHz, 22 °C, C_6D_6/THF-d_8): δ 3.12 (s, 6H, DME), 3.31 (s, 4H, DME). $^{19}F\{^1H\}$ NMR (470 MHz, 22 °C, C_6D_6/THF-d_8): δ −116.16 (br s, 2F, *p*-F), −106.42 (br s, 4F, *m*-F), −102.42 (d, 4F, $^3J_{FF}$ = 12.1 Hz, *o*-F). IR (KBr pellet, cm^{-1}): 3435 (w), 2959 (w), 2673 (w), 2473 (w), 1652 (w), 1628 (w), 1516 (s), 1485 (s), 1372 (w), 1315 (w), 1250 (w), 1179 (m, ν_{CO}), 1167 (m), 1085 (m), 1025 (s), 997 (s), 935 (m, ν_{asym}U=O), 864 (m), 656 (m), 479 (m), 463 (m), 431 (m).

Synthesis of $C_6F_5{}^{18}OH\cdot0.5DME$. The synthesis of $C_6F_5{}^{18}OH$ was adapted from a previously reported procedure.[113] To a 100 mL Schlenk flask equipped with a reflux condenser were added KH (0.350 g, 8.54 mmol) and DME (20 mL). The suspension was cooled to −78 °C, and $H_2{}^{18}O$ (0.22 mL, 11.0 mmol) was added dropwise. The mixture was allowed to warm to room temperature, and C_6F_6 (0.5 mL, 4.33 mmol) was added, whereupon the reaction mixture was refluxed for 15 h. Upon cooling, the solution was filtered, and the DME was removed in vacuo yielding $[K(DME)_x][{}^{18}OC_6F_5]$ as a white solid. This solid was subsequently dissolved in Et_2O (10 mL) and treated with HCl (3.5 mL, 1 M in Et_2O). The resulting suspension was filtered through a Celite column (3 cm × 2 cm) supported on a glass frit, and the filtrate was removed in vacuo yielding $C_6F_5{}^{18}OH\cdot0.5DME$ as a white solid. 0.450 g, 45% yield. ^1H NMR (400 MHz, 22 °C, C_6D_6): δ 3.07 (s, 3H, DME), 3.26 (s, 2H, DME), 4.50 (s, 1H, OH). $^{19}F\{^1H\}$ NMR (470 MHz, 22 °C, C_6D_6): δ −107.43 (triplet of triplets, 1F, $^3J_{FF}$ = 22.5 Hz, $^4J_{FF}$ = 6.2 Hz, *p*-F), −102.54 (t, 2F, $^3J_{FF}$ = 20.4 Hz, *m*-F), −101.24 (dd, 2F, $^3J_{FF}$ = 18.1 Hz, $^4J_{FF}$ = 5.5 Hz, *o*-F). MS (EI): *m*/*z* 186 ($H^{18}OC_6F_5$), 155 (C_5F_5), 136 (C_5F_4), 117 (C_5F_3), 105 (C_4F_3), 93 (C_3F_3), 86 (C_4F_2), 69 (CF_3).

$UO_2({}^{18}OC_6F_5)_2(DME)$ (5-^{18}O). To a solution of $U(O^tBu)_6$ (0.035 g, 0.052 mmol) in hexanes (5 mL) was added $C_6F_5{}^{18}OH\cdot0.5DME$ (0.073 g, 0.316 mmol) dissolved in hexanes (1 mL). The resulting dark-red solution gradually lightened over the course of 12 h, affording a red-orange solution concomitant with the deposition of an orange powder. The supernatant was decanted off, and the powder was washed with hexanes (2 × 2 mL) and dried under vacuum: 0.021 g, 55% yield. ^1H NMR (500 MHz, 22 °C, C_6D_6/THF-d_8): δ 3.15 (s, 6H, DME), 3.31 (s, 4H, DME). $^{19}F\{^1H\}$ NMR (470 MHz, 22 °C, C_6D_6/THF-d_8): δ −113.94 (br s, 2F, *p*-F), −105.21 (t, 4F, $^3J_{FF}$ = 21.4 Hz, *m*-F), −102.32 (d, 4F, $^3J_{FF}$ = 18.0 Hz, *o*-F). IR (KBr pellet, cm^{-1}): 3424 (w), 2959 (w), 2665 (w), 2460 (w), 1652 (w), 1628 (w), 1513 (s), 1478 (s), 1372 (w), 1313 (w), 1250 (w), 1169 (m), 1158 (m, ν_{CO}), 1085 (m), 1021 (s), 994 (s), 935 (m, ν_{asym}U=O), 864 (m), 642 (m), 475 (m), 462 (m), 419 (m).

$U(O^tBu)_2(OC_6F_5)_4$ (6). To a stirring solution of $U(O^tBu)_6$ (0.015 g, 0.022 mmol) in pentane (3 mL) was added C_6F_5OH (0.041 g, 0.227 mmol) dissolved in pentane (1 mL). The solution immediately turned dark-red. The solvent was then removed in vacuo to yield a black solid, which was redissolved in pentane (3 mL) and stored at −25 °C for 3 days. This resulted in the deposition of a few dark-red crystals, which were collected and dried under vacuum. The solid-state molecular structure was determined by X-ray crystallographic analysis. Subsequent attempts to reproduce this material for further characterization were unsuccessful.

$[Li(DME)_3]_2[U(OC_6F_5)_6]$ (7). To a solution of $[Li(THF)]_2[U(O^tBu)_6]$ (0.200 g, 0.240 mmol) in diethyl ether (5 mL) was added C_6F_5OH (0.441 g, 2.400 mmol) dissolved in diethyl ether (1 mL). The solution immediately turned green-amber. After stirring for 4 h the solvent was removed in vacuo to yield an amber oil. Addition of DME (5 mL), followed by stirring for 1 h, resulted in the formation of a pale-pink powder. The pale-pink powder was subsequently washed with hexanes (3 × 4 mL). The powder was redissolved in diethyl ether (9 mL) and DME (0.5 mL) and layered with hexanes (9 mL). This solution was stored at −25 °C for 48 h to yield a pale-pink crystalline solid, which was washed with hexanes (4 mL) and dried under vacuum: 0.176 g, 81% yield. Crystals of **7** turned opaque and pale-blue upon application of vacuum. ^1H NMR (400 MHz, 22 °C, CD_2Cl_2): δ 2.42 (br s, 24H, DME), 3.02 (s, 36H, DME). $^7Li\{^1H\}$ NMR (194 MHz, 22 °C, CD_2Cl_2): δ −22.55 (br s). $^{19}F\{^1H\}$ (376 MHz, 22 °C, CD_2Cl_2): δ −111.50 (s, 6F, *p*-F), −107.84 (s, 12F, *m*-F), −105.22 (s, 12F, *m*-F). Anal. Calcd for $[Li(DME)_3]_2[U(OC_6F_5)_6]$, $C_{60}H_{60}F_{30}Li_2O_{18}U$: C, 38.11; H, 3.20. Anal. Calcd for $[Li(DME)]_2[U(OC_6F_5)_6]$, $C_{44}H_{20}F_{30}Li_2O_{10}U$: C, 34.53; H, 1.32. Found: C, 34.14; H, 1.34.

$[Li(DME)_3][U(OC_6F_5)_6]$ (8). To a solution of **7** (0.150 g, 0.080 mmol) in CH_2Cl_2 (7 mL) was added AgOTf (0.041 g, 0.160 mmol). The reaction mixture immediately turned dark-red. Stirring was continued for 24 h at room temperature. The solution was then filtered through a Celite column (2 cm × 0.5 cm) supported on glass wool, affording a dark-red filtrate. The filtrate was layered with hexanes (10 mL) and stored at −25 °C for 24 h, which resulted in the deposition of dark-red crystals. The solid was washed with hexanes (3 × 4 mL) and dried under vacuum: 0.103 g, 81% yield. ^1H NMR (400 MHz, 22 °C, CD_2Cl_2): δ 3.43 (s, 18H, DME), 3.60 (s, 12H, DME). $^7Li\{^1H\}$ NMR (194 MHz, 22 °C, CD_2Cl_2): δ −1.90 (s). $^{19}F\{^1H\}$ (376 MHz, 22 °C, CD_2Cl_2): δ −105.19 (t, 6F, $^3J_{FF}$ = 21.3 Hz, *p*-F), −104.16 (t, 12F, $^3J_{FF}$ = 16.8 Hz, *m*-F), −99.03 (d, 12F, $^3J_{FF}$ = 11.6 Hz, *o*-F). Anal. Calcd for $C_{48}H_{30}F_{30}LiO_{12}U$: C, 35.73; H, 1.88. Found: C, 35.35; H, 2.02.

$[Ag(\eta^2\text{-}C_7H_8)_2(DME)][U(OC_6F_5)_6]$ (9). To a stirring solution of **7** (0.210 g, 0.111 mmol) in toluene (4 mL) was added AgOTf (0.071 g, 0.276 mmol). The reaction mixture immediately turned dark-red. Stirring was continued for 12 h at room temperature, whereupon the solution was filtered through a Celite column (2 cm × 0.5 cm) supported on glass wool, affording a dark-red filtrate. The solvent was removed in vacuo to give a tacky red solid. The solid was redissolved in toluene (4 mL) and again filtered through a Celite column (2 cm × 0.5 cm). The filtrate was layered with hexanes (10 mL) and stored at −25 °C for 12 h, resulting in the deposition of dark-red crystals. The solid was washed with hexanes (3 × 4 mL) and dried under vacuum: 0.180 g, 60% yield. Crystals of **9** turned opaque upon application of vacuum. ^1H NMR (400 MHz, 22 °C, CD_2Cl_2): δ 2.37 (s, 6H, toluene CH_3), 3.45 (s, 6H, DME), 3.62 (s, 4H, DME), 7.19 (m, 2H, toluene CH), 7.25 (m, 4H, toluene CH), 7.30 (m, 4H, toluene CH). $^{19}F\{^1H\}$ (376 MHz, 22 °C, CD_2Cl_2): δ −105.15 (t, 6F, $^3J_{FF}$ = 20.7 Hz, *p*-F), −104.13 (t, 12F, $^3J_{HH}$ = 16.0 Hz, *m*-F), −98.99 (d, 12F, $^3J_{FF}$ = 13.0 Hz, *o*-F). Anal. Calcd for $[Ag(\eta^2\text{-}C_7H_8)_2(DME)][U(OC_6F_5)_6]$, $C_{54}H_{26}AgF_{30}O_8U$: C, 37.73; H, 1.53. Anal. Calcd for $[Ag(\eta^2\text{-}C_7H_8)(DME)][U(OC_6F_5)_6]$, $C_{47}H_{18}AgF_{30}O_8U$: C, 34.71; H, 1.12. Found: C, 34.76; H, 1.43.

(113) Pummer, W. J.; Wall, L. A. *Science* **1958**, *127*, 643–644.

Table 1. X-ray Crystallographic Data for Complexes **3**, **4**, **6**, **7**, and **9**

	3	**4**	**6**	**7**	**9**
empirical formula	$C_{44}H_{20}F_{30}LiO_8U$	$C_{20}H_{20}F_{10}O_6U$	$C_{32}H_{18}F_{20}O_6U$	$C_{60}H_{60}F_{30}Li_2O_{18}U$	$C_{54}H_{26}AgF_{30}O_8U$
crystal habit, color	irregular,dark-red	needle, red	prism, dark-red	cube, clear	block, red
crystal size (mm)	0.3 × 0.2 × 0.08	0.7 × 0.1 × 0.1	0.5 × 0.2 × 0.02	0.2 × 0.2 × 0.14	0.6 × 0.4 × 0.2
crystal system	triclinic	monoclinic	triclinic	rhombohedral	triclinic
space group	$P\bar{1}$	$C2/c$	$P\bar{1}$	$R\bar{3}$	$P\bar{1}$
volume (Å^3)	2487.7(7)	2509.7(4)	885.8(8)	5441(2)	2804(1)
a (Å)	11.006(2)	12.665(1)	10.147(5)	15.738(2)	11.808(3)
b (Å)	11.949(2)	19.327(2)	10.565(5)	15.738(2)	12.910(3)
c (Å)	20.903(3)	11.132(1)	10.637(5)	25.277(7)	19.626(4)
α (°)	94.746(2)	90	68.547(7)	90	82.199(3)
β (°)	90.733(2)	112.922(3)	63.240(7)	90	79.196(3)
γ (°)	114.593(2)	90	62.611(6)	120	73.259(3)
Z	2	4	1	3	2
formula weight (g/mol)	1491.57	784.39	1116.49	1890.99	1718.65
density (calculated) (Mg/m^3)	1.991	2.076	2.093	1.741	2.036
absorption coefficient (mm^{-1})	3.427	6.575	4.731	2.393	3.389
F_{000}	1426	1480	530	2796	1646
total no. reflections	19 511	9661	5948	9817	23 446
unique reflections	9423	2669	3319	2500	11 227
final R indices ($I > 2\sigma(I)$]	$R_1 = 0.0488$, $wR_2 = 0.1066$	$R_1 = 0.0479$, $wR_2 = 0.1233$	$R_1 = 0.0631$, $wR_2 = 0.1392$	$R_1 = 0.0367$ $wR_2 = 0.0716$	$R_1 = 0.0439$, $wR_2 = 0.1039$
largest diff. peak and hole (e$^-$ Å^{-3})	1.596 and −0.752	3.426 and −1.285	4.218 and −1.690	0.711 and −0.353	1.534 and −1.015
GOF	0.901	1.053	0.997	0.914	0.926

UV−vis/NIR (toluene, 4.95 mmol, 25 °C): 776 (ε = 29.9 L·mol^{-1}·cm^{-1}), 876 (ε = 23.4 L·mol^{-1}·cm^{-1}), 948 (ε = 20.5 L·mol^{-1}·cm^{-1}), 1368 (ε = 4.25 L·mol^{-1}·cm^{-1}), 1424 (ε = 26.6 L·mol^{-1}·cm^{-1}).

X-ray Crystallography. Data for **3**, **4**, **6**, **7**, and **9** were collected on a Bruker three-axis platform diffractometer equipped with a SMART-1000 CCD detector using a graphite monochromator with a Mo Kα X-ray source (α = 0.71073 Å). The crystals were mounted on a glass fiber under Paratone-N oil and all data collected at 150(2) K using an Oxford nitrogen gas cryostream system. A hemisphere of data was collected using ω scans with 0.3° frame widths. Frame exposures of 20, 15, 25, 30, and 15 s were used for complexes **3**, **4**, **6**, **7**, and **9**, respectively. Data collection and cell parameter determination were conducted using the SMART program.[114] Integration of the data frames and final cell parameter refinement were performed using SAINT software.[115] Absorption correction of the data was carried out empirically based on reflection Ψ-scans. Subsequent calculations were carried out using SHELXTL.[116] Structure determination was done using direct or Patterson methods and difference Fourier techniques. All hydrogen atom positions were idealized and rode on the atom of attachment with exceptions noted in the subsequent paragraph. The structure solution, refinement, graphics, and creation of publication materials were performed using SHELXTL.[116]

Structure **4** possessed disorder about the tertiary carbon of the *tert*-butoxide groups. The ligand disorder was addressed by assigning the groups in two positions, and occupancy was determined through data refinement. Restraints were applied to the disordered *tert*-butoxide groups by fixing the C−C bond lengths between the tertiary and methyl carbons to 1.50(1) Å, and constraining the involved C atom to have ideal tetrahedral geometry. Idealized hydrogens were not assigned to the disordered carbons or *tert*-butanol oxygen atoms. A summary of relevant crystallographic data for **3**, **4**, **6**, **7**, and **9** is presented in Table 1.

Acknowledgment. We thank the University of California, Santa Barbara, for financial support of this work.

Supporting Information Available: X-ray crystallographic details (as CIF files) of **3**, **4**, **6**, **7**, and **9**. Tabulated cyclic voltammetry data for **1**, **2**, and **7**. IR spectra of **5** and **5-^{18}O**. Selected NMR spectra of **1**−**5** and **7**−**9**. This material is available free of charge via the Internet at http://pubs.acs.org.

IC802266Y

(114) *SMART Software User's Guide*, Version 5.1; Bruker Analytical X-ray Systems, Inc.: Madison, WI, 1999.
(115) *SAINT Software User's Guide*, Version 5.1; Bruker Analytical X-ray Systems, Inc.: Madison, WI, 1999.
(116) Sheldrick, G. M. *SHELXTL, 6.12*; Bruker Analytical X-ray Systems, Inc.: Madison, WI, 2001.